Journal of Advanced Ceramics
2020, **9**(1): 1–16
https://doi.org/10.1007/s40145-019-0332-6

ISSN 2226-4108
CN 10-1154/TQ

Review

Sol–gel derived porous ultra-high temperature ceramics

Fei LI[a,*], Xiao HUANG[b], Ji-Xuan LIU[a], Guo-Jun ZHANG[a,*]

[a]*State Key Laboratory for Modification of Chemical Fibers and Polymer Materials*, *Institute of Functional Materials*, *Donghua University*, *Shanghai 201620*, *China*
[b]*Institute for the Conservation of Cultural Heritage*, *Shanghai University*, *Shanghai 200444*, *China*

Received: December 20, 2018; Revised: April 10, 2019; Accepted: April 15, 2019

Abstract: Ultra-high temperature ceramics (UHTCs) are considered as a family of nonmetallic and inorganic materials that have melting point over 3000 ℃. Chemically, nearly all UHTCs are borides, carbides, and nitrides of early transition metals (e.g., Zr, Hf, Nb, Ta). Within the last two decades, except for the great achievements in the densification, microstructure tailoring, and mechanical property improvements of UHTCs, many methods have been established for the preparation of porous UHTCs, aiming to develop high-temperature resistant, sintering resistant, and lightweight materials that will withstand temperatures as high as 2000 ℃ for long periods of time. Amongst the synthesis methods for porous UHTCs, sol–gel methods enable the preparation of porous UHTCs with pore sizes from 1 to 500 μm and porosity within the range of 60%–95% at relatively low temperature. In this article, we review the currently available sol–gel methods for the preparation of porous UHTCs. Templating, foaming, and solvent evaporation methods are described and compared in terms of processing–microstructure relations. The properties and high temperature resistance of sol–gel derived porous UHTCs are discussed. Finally, directions to future investigations on the processing and applications of porous UHTCs are proposed.

Keywords: sol–gel; ultra-high temperature ceramics; porous ceramics; processing; microstructure

1 Introduction

Ultra-high temperature ceramics (UHTCs) are a class of nonmetallic and inorganic materials that have melting point over 3000 ℃ and are typically borides, carbides, and nitrides of early transition metals (e.g., Zr, Hf, Nb, Ta) [1–8]. Due to the combination of series of excellent physical and chemical properties, such as high hardness, good high-temperature stability, and excellent solid-phase stability, UHTCs are considered as promising candidate materials for high-temperature structural applications, including engines, hypersonic vehicles, plasma arc electrode, cutting tools, furnace elements, and high-temperature shielding [7,9–13]. UHTCs are difficult to densify without sintering additives and external pressure. Numerous researches have been made in recent decades for the synthesis and densification of UHTCs at moderate conditions and further enhancements of their performance [14]. One of the potential applications for porous UHTCs is used as thermal insulating materials in thermal protection systems of reusable launch vehicles, which experience extreme high temperatures (> 2000 ℃) during high-

*Corresponding authors.
E-mail: F. Li, lifei80380@163.com;
G. Zhang, gjzhang@dhu.edu.cn

speed cruise. Few materials can meet this criterion. The maximum using temperature for typical rigid tiles (e.g., alumina-enhanced thermal barrier, AETB) is ~1600 ℃ [15]. Recent interest in UHTCs has been motivated by the search for materials that can withstand extreme environments over 2000 ℃. UHTCs possess excellent phase stability at high temperatures. Hopefully, pores are introduced in UHTCs to give out novel and lightweight thermal insulating materials.

Many researchers focused on the preparation of porous UHTCs, aiming to develop high-temperature resistant, sintering resistant, and lightweight materials [16–23]. In the late 1990s, NASA and Aspen Systems proposed a Phase I project to develop ultra-high temperature resistant zirconium and hafnium carbide aerogels. They would use their expertise in aerogel manufacturing and sol–gel science to develop a low-temperature process for the production of refractory carbide aerogels. However, no further open reports or publications can be reached. In March 2013, Prof. Franks and Dr. Tallon from the University of Melbourne started a two-and-a-half-year project on "multi-scale porous ultra-high temperature ceramics" funded by the Asian Office of Aerospace Research and Development (AOARD) [16]. The object of this project was to develop highly porous UHTCs that can be potentially used in insulation packages for ultra-high temperature applications. Processing conditions were investigated and then optimized to prepare zirconium diboride porous materials with up to 92% porosity by replica, particle stabilized foams, ice templating, and partial sintering methods. In August 2016, Prof. Ireland from University of Oxford and partners from University of Birmingham, Imperial College London, and University of Southampton started a five-year project entitled "transpiration cooling systems for jet engine turbines and hypersonic flight" funded by Engineering and Physical Sciences Research Council (EPSRC) [24]. One of their research topics was to develop UHTCs (zirconium diboride) with controlled porosity to be used as a key component in transpiration cooling systems for hypersonic flights. In January 2017, Dr. Li from Donghua University started a three-year project funded by National Natural Science Foundation of China (NSFC) to develop porous zirconium carbide foams by direct foaming methods [22]. However, very limited papers on the preparation and application of porous UHTCs can be found [17,18,21–23,25–27].

The processing routes used for the production of porous ceramics can be categorized as partial sintering, replica method, sacrificial template method, and direct foaming method [28–32]. It is important to get a well dispersed ceramic slurry or liquid precursor for the fabrication of porous ceramics with tailored microstructure and chemical composition [33–35]. Porous UHTCs can be obtained by using ceramic powders as raw materials, followed by colloidal processing (e.g., freeze casting, gel casting, and foaming) of the ceramic slurry, shaping, and pressureless sintering [17,18,27]. The sintering temperature (1800–2100 ℃) is selected to allow for particle necking to provide good mechanical strength, but not high enough to get full densification of the particles in the skeletons [16]. These powder-derived porous UHTCs are not sintering-resistant. At higher temperatures, grain coarsening leads to the formation of large grains, indicating poor high-temperature stability [36]. Large grains often result in a degradation in strength.

An alternative way to prepare porous UHTCs is to use the liquid sols which contain transition metal salts, boron source, and organic carbon source as raw materials [21–23,25]. After sol–gel reactions, shaping with specific techniques, drying at moderate conditions, and pyrolysis at high temperatures, the porous UHTCs with desired compositions are obtained. Numbers of papers focus on the design and pyrolysis of UHTCs precursors to fine UHTCs powders through sol–gel methods [37]. However, rare works have been published on sol–gel derived porous monolithic UHTCs. These porous UHTCs are expected as thermal resistant materials at extreme high temperatures, and also should be able to bear loadings in some cases. Evaluation of the porous UHTCs should be based on high-temperature stability (e.g., dimensional, microstructure, thermal expansion), mechanical property, thermal conductivity, and thermal shock resistance, etc.

Some excellent reviews and papers concerning the sol–gel derived porous monoliths are available [29,38, 39]. However, few papers focusing on the preparation of non-siliceous especially UHTCs monoliths from sol–gel methods can be found. The aim of this article is to summarize and compare some of the sol–gel processing routes currently available for the preparation of porous monolithic UHTCs, including porous ZrC-, HfC-, and ZrB_2-based ceramics. The synthesis of UHTCs powders from sol–gel or liquid precursor routes will not be discussed here. Sacks *et al*. [40], Dollé *et al*. [41], Yan *et al*. [42], Ang *et al*. [43], Cai *et al*. [44], and

Li *et al*. [37] are suggested for those interested in these research topics.

2 Processing–microstructure relations

2. 1 General features of porous UHTCs via sol–gel process

Sol–gel is a very powerful technique for the synthesis of wide range materials [29,38,45,46]. It is generally involved with the mixing of chemicals in a solution, gelation, drying, and post-treatment to obtain final products [29]. Starting from a homogeneous liquid state, nanopowders, fibers, films, and porous monoliths with tailored structure can be made from sol–gel routes combined with various drying and shaping techniques. Beginning a synthesis in the liquid state, in which all starting reagents are mixed at molecular level, can also result in lower synthesis temperatures [43,47]. A large variety of parameters, such as the choice of the precursors, its concentration, temperature, solvent, etc., have significant influence on the composition, microstructure, and properties of the sol–gel derived materials [29,38]. Heat treatment is important for drying gels as well as the converting organic/inorganic hybrid gels to ceramics [48]. Drying of the gels during which the solvent between gel network is removed by evaporation or sublimation is a critical step in synthesizing monoliths. Shrinking, cracking, and collapse of the gels caused by surface tension are very common in sol–gel processing, which make it often difficult to prepare large monolithic materials [29,48]. Powders and cracked fragments are often obtained in sol–gel processing of UHTCs, as shown in Fig. 1 [41,49]. Special drying techniques such as supercritical drying and freeze drying, as well as other strategies like surface modification, exhausted solvent-exchange or combinations of these techniques have been developed to weaken the capillary forces during drying to obtain monolithic pieces [29,45,50–52].

In the case of sol–gel processing of porous UHTCs, the preparation methods can roughly be divided in three categories according to how the porous structures are formed in the green body: templating method, foaming method, solvent evaporation method, as schematically illustrated in Fig. 2. The templating method involves the impregnation and infiltration of a porous structure (as template) with the preceramic sol [49,53]. After the impregnation and infiltration process, the green body is first dried and then heated at temperatures up to 1600 ℃ for the formation of porous UHTCs via carbothermal reduction reaction. The porous UHTCs exhibit almost the same morphology as the original porous template but with some extent of shrinkage. The use of porous structure as template is an

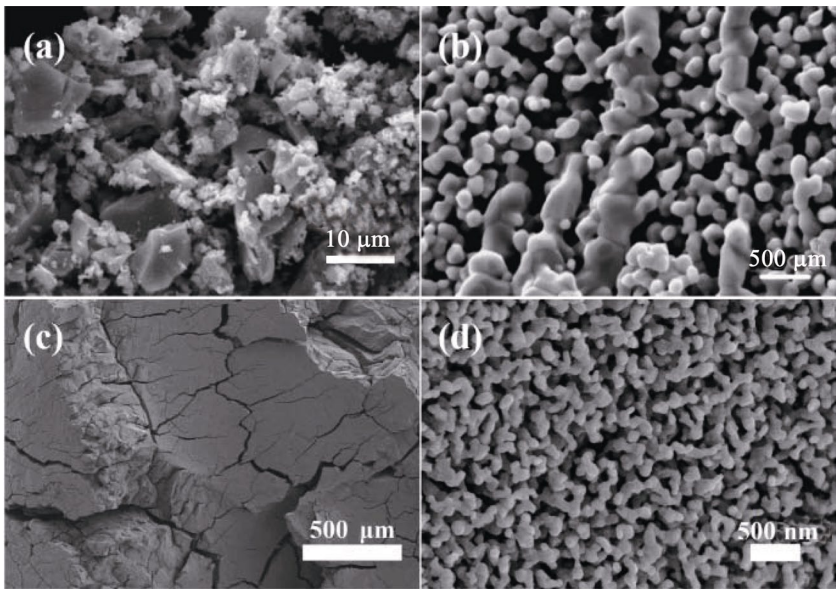

Fig. 1 SEM images of sol–gel derived ZrC powders heated (a) at 1600 ℃ for 3 h and (b) at 1400 ℃ for 2.5 h then at 1800 ℃ for 6 min. Reproduced with permission from Ref. [41], © Elsevier Ltd. 2006. (c) Low and (b) high magnification SEM images of sol–gel derived ZrC/SiC composite heated at 1500 ℃ for 1 h [49]. Reproduced with permission from Ref. [49], © Springer Science+Business Media, LLC, part of Springer Nature 2018.

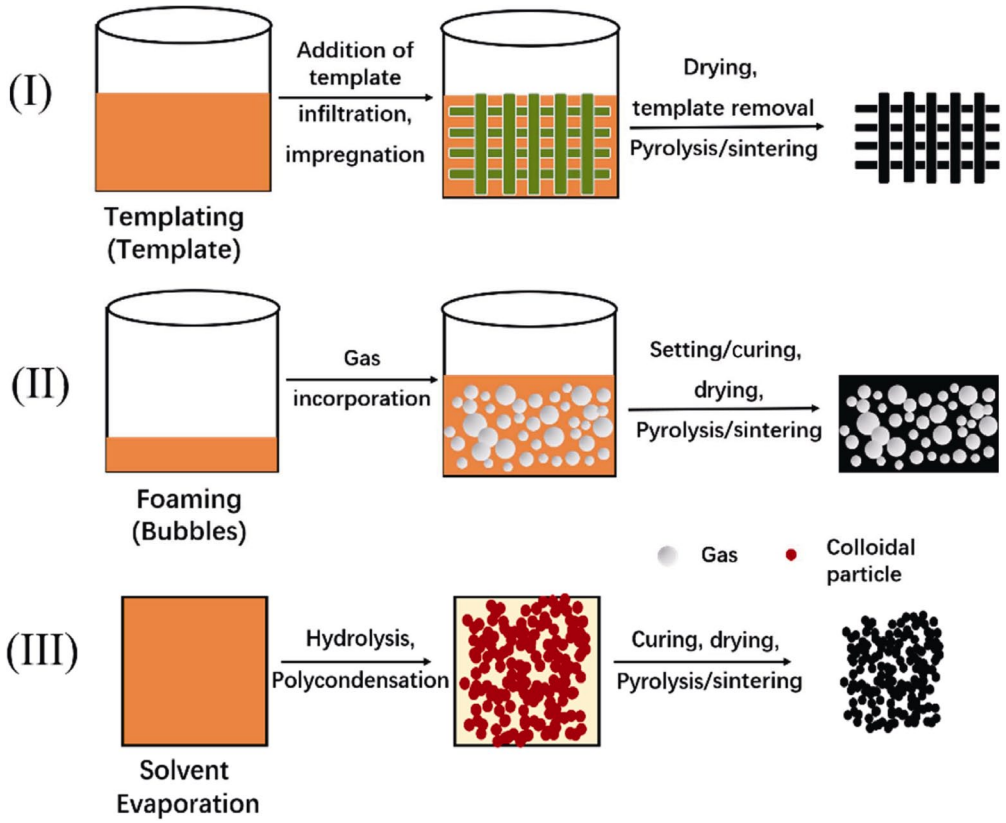

Fig. 2 Scheme of sol–gel methods for the preparation of porous UHTCs.

important feature for this method. In the foaming methods, bubbles are first generated by introducing air or volatile reagents into the preceramic sol, then are set to obtain foamed green body [23,25]. The foamed green body is afterwards heated at high temperatures to obtain porous UHTCs. Bubble generation and stabilization are the characteristic features of this foaming method. In solvent evaporation methods, which is template free, the preceramic sol undergoes sol–gel transition to form a monolithic wet gel, which contains a continuous solid network enclosing a continuous liquid phase [21,22]. The solvent between the solid network evaporates out by heat treatment and pores are left behind in the organic/inorganic hybrid gels. Consequently, the porous hybrid gels are pyrolyzed at high temperatures to obtain porous UHTCs. No porous templates are used and no bubbles are generated in this solvent evaporation method.

In sol–gel derived porous UHTCs, which started from liquid precursors, heat treatment at temperatures up to 1300–1600 ℃ in inert atmosphere was necessarily required to convert the preceramic gels into UHTCs composition [41,54–56]. Figure 3 shows the typical TG–DSC curves of the dried gel in inert gas flow at 40 to 1600 ℃ and the XRD patterns of the pyrolyzed products at various temperatures [21]. These results demonstrated that the UHTCs phases started to form at 1200 ℃ and completed at temperatures from 1300 to 1500 ℃ accompanied by a huge weight loss.

A number of porosities and pore sizes have been produced by these methods for ZrC, ZrC/SiC, ZrB_2, and ZrB_2/SiC, etc. [21–23,25,53,57]. Figure 4 is a map of porosities–pore sizes–applications of several groups of porous materials [30]. And the locations of the sol–gel derived porous UHTCs are also shown in Fig. 4. The pore sizes of the sol–gel derived porous UHTCs are relatively small when compared with the porous materials with similar porosity level. Such features demonstrate that the sol–gel derived porous UHTCs may find applications as high temperature resistant thermal insulators.

Table 1 lists the characteristics of the porous UHTCs made from various processing methods. All these processing methods can be used to prepare porous UHTCs with porosities over 70%. Templating methods are simple and easy to handle with, and can be used to prepare porous UHTCs that mimicking templates. Foaming methods are suitable for the synthesis

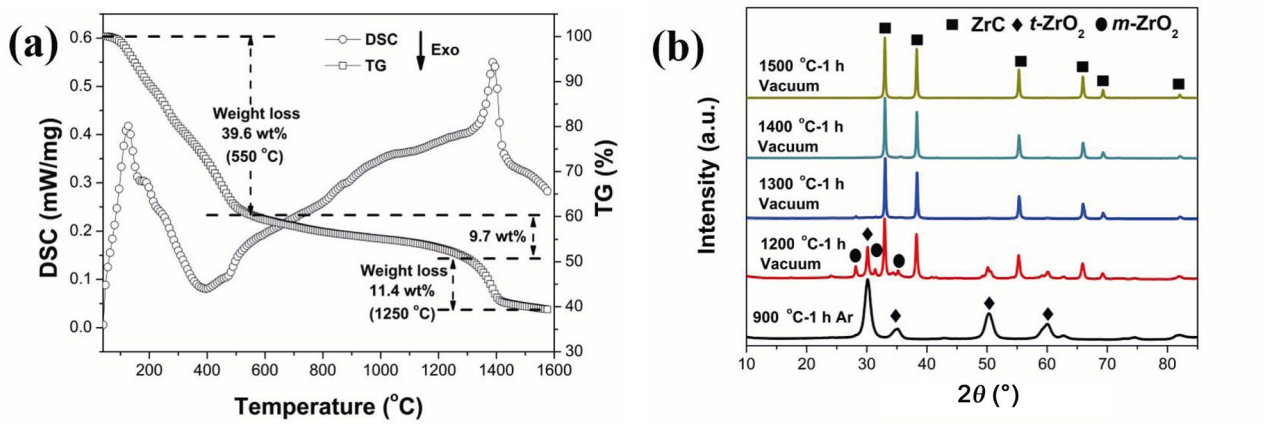

Fig. 3 (a) Typical TG–DSC curves of the dried gel in argon flow [21]. Reproduced with permission from Ref. [21], © Elsevier Ltd. 2018. (b) XRD patterns of the products obtained from pyrolyzing the dried gels at various temperatures [21]. Reproduced with permission from Ref. [21], © Elsevier Ltd. 2018.

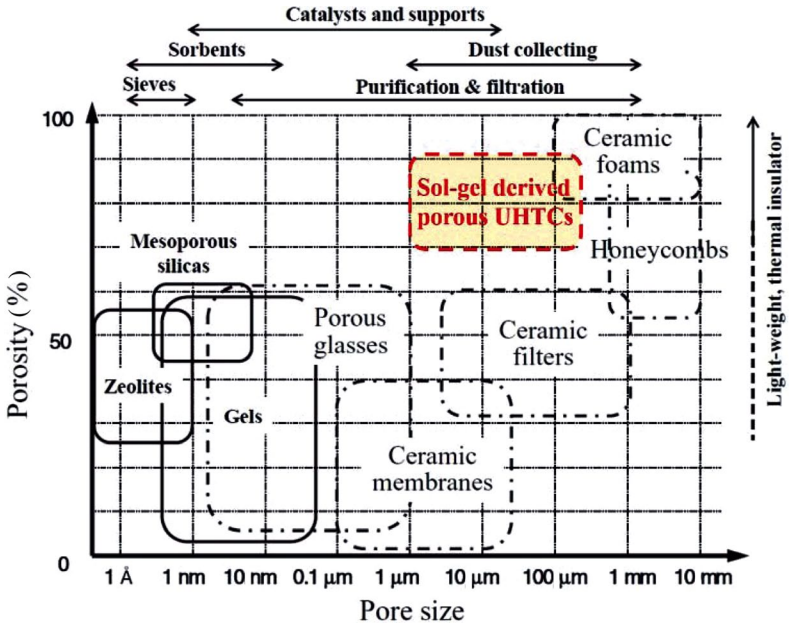

Fig. 4 Pore size and porosity of typical porous substances and ceramics [30]. Reproduced with permission from Ref. [30], © National Institute for Materials Science 2011.

Table 1 Characteristics of the porous UHTCs made from various processing methods

Composition	Method	Porosity	Pore size (μm)	Type of the pores	Compressive strength (MPa)
ZrC/C [53]	Sol–gel, templating	78%	~20	Open	—
ZrC/SiC [49]	Sol–gel, templating	78.1%	80–200	Open	0.4–0.67
ZrC/C [23]	Sol–gel, foaming	85%	~40	Closed cell	0.4
ZrC [25]	Sol–gel, foaming	67.6%–93%	100–300	Open & closed	0.15
ZrB_2/ZrC/SiC [22]	Sol–gel, solvent evaporation	74.3%–82%	1.0–10	Open	1.2–1.9
ZrC/SiC [21]	Sol–gel, solvent evaporation	~70%	3–16	Open	0.3–0.7
ZrB_2/SiC [17]	Camphene-based freeze casting	10%–60%	200–300	Open	173–364
ZrB_2 [18]	Ice templating	48%–57%	20–180	Layered structure	18–68
ZrB_2 [36]	Gel casting	55%	~220	Open	79
ZrB_2/SiC [58]	Partial sintering	2%–35%	1.4–5.5	Open	—

of porous UHTCs with tailored open and closed cell structures. Solvent evaporation methods are suitable for the synthesis of porous UHTCs with pore sizes down to 1–20 μm and with relatively high compressive strength. Porous UHTCs made by sol–gel methods possess high porosity and small pore size but with low compressive strength. Porous UHTCs made by gel casting, freeze casting, and partial sintering are strong but with relatively low porosities. Such statements are added in the revised manuscript.

2. 2 Templating methods

Since invented by Schwartzwalder *et al.* [59] in 1963, templating methods have been simple and versatile ways to prepare porous ceramic products by using the natural or synthetic templates as skeletal supporting structure [31]. The great flexibility of the templating method is partly due to the fact that it is applicable to any ceramic material that can be appropriately dispersed into a slurry or a sol. The microstructures of template-derived porous ceramics depend primarily on the porous structure of the templates. However, there are only a few reports about the synthesis of cellular zirconium carbide and its composite in current literature. Rambo *et al*. [53] used wood templating method to prepare porous ZrC/C ceramics with porosity of 78%. The zirconia sol or colloidal suspension was prepared by hydrolysis and condensation of zirconium *n*-propoxide. Zirconia sol was vacuum infiltrated into the pine wood derived carbon template and was subsequently dried to obtain a zirconia gel coated porous wood structure. The infiltration and drying processes were carried out four times to reach a high zirconia content. Zirconia gel was converted into ZrO_2 and then reacted with the wood derived carbon template to form ZrC phase upon pyrolysis. The original pine char microstructure was reproduced in the porous ZrC/C ceramic. Island-like ZrC particles were observed on the cell walls and in the channels, as shown in Fig. 5.

In the wood derived porous UHTCs, in which the wood derived carbon templates also play the role as carbon source, it is difficult to produce near stoichiometric porous structures [53]. High residual carbon yield in the final ceramic composition seems to be characteristic feature for this wood templating method. The maximum achievable ZrC phase content was lower than 20 vol% in Ref. [53]. The initial porosity of the biocarbon template and the amount of infiltrated preceramic precursor are crucial for the conversion ratio of metal oxide to metal carbide. The sol viscosity also plays a key role in the templating method [31,53]. Started from high viscosity sol, a non-homogeneity of the sol-infiltration and the clogging of

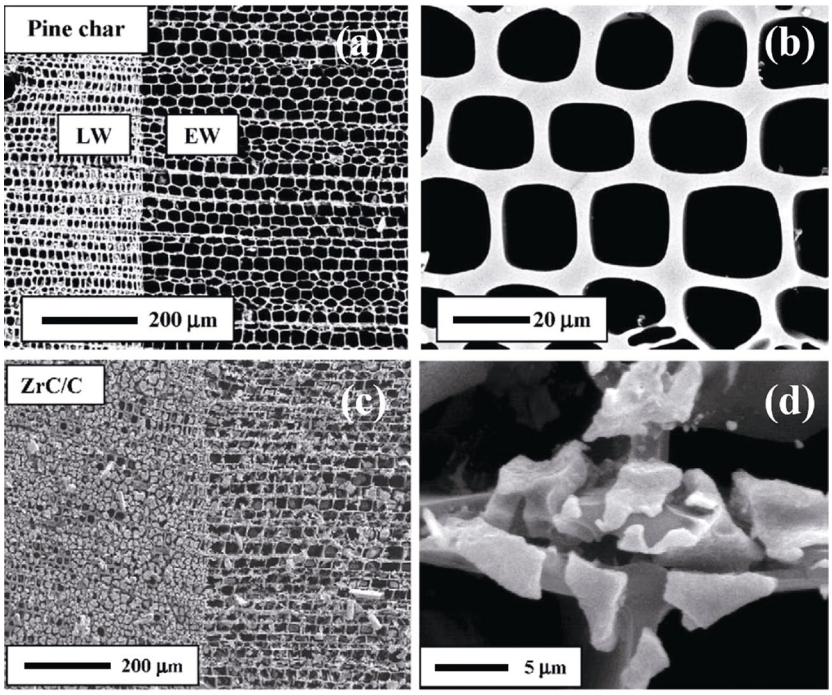

Fig. 5 SEM images of the pine wood char with (a) low and (b) high magnifications. SEM images of the wood derived porous ZrC/C with (c) low and (d) high magnifications [53]. Reproduced with permission from Ref. [53], © Elsevier Ltd. 2005.

the pores after multiple infiltration and drying cycles result in low ceramic content and inhomogeneous structures in the final porous products.

The low viscosity sol facilitates the entrance to the porous structures much more easily, and may allow higher weight gain during the cycling infiltration. Wood derived carbon templates are rigid and do not suffer from distortion or deformation during infiltration and drying processes; however, soft or flexible templates (e.g., polymeric sponge, melamine foam) do. Li *et al.* [49] reported the preparation of ZrC/SiC foam by using melamine foam as template. They infiltrated furfuryl alcohol/polyzirconoxane/tetraethyl orthosilicate (FA/PZO/TEOS) derived hybrid sols into melamine foam to get a hybrid foam. The hybrid sol can be converted into the desired ceramic composition upon drying and pyrolysis with no extra carbon source is required. When impregnated with high viscosity sol, the as-dried hybrid foam showed twisted sides probably caused by the inhomogeneous sol infiltration and gel shrinkage, as shown in Figs. 6(a) and 6(b). The hybrid foam underwent nearly 10% linear shrinkage accompanied by gel shrinkage during drying. While treated with low viscosity hybrid sol, the original rectangular shape of the melamine foam was well retained, as shown in Fig. 6(c). These hybrid foams were converted into open-cell structured ZrC/SiC foams after heat treatment at 1500 ℃ (Figs. 6(d) and 6(e)). The porous ZrC/SiC obtained with the melamine template method can reach open porosity of 78.1% and possess a monomodal pore size distribution between 80 and 200 μm.

2. 3 Foaming methods

Bubble stabilization in the wet foam is the critical issue in foaming methods, and plays a key role in controlling the porous structures of the final ceramic products [31,60–62]. Bubbles can be generated by introducing air or volatile reagents into a colloidal suspension or viscous liquid via strong mechanical mixing. The wet bubbles can be stabilized by rapid crosslinking/ gelation of the solid skeletons, and stabilized with the help of surfactants and particles at the interfaces. The consolidated foams are afterwards heated at high temperatures to obtain porous ceramics. We describe below the foaming methods currently available on synthesis of porous UHTCs.

Li e*t al.* [23] prepared ZrC/C foams by direct foaming the mixtures of foamable phenolic resin and zirconia sol. Volatile pentane is used as foaming agent. The stabilization of the bubbles is mainly due to the thermal setting of phenolic resin. By pyrolyzing the foamed green body at 1600 ℃, highly porous ZrC/C foam was prepared (Figs. 7(a) and 7(b)). The density and porosity of ZrC/C foam were 0.16–0.19 g/cm^3 and

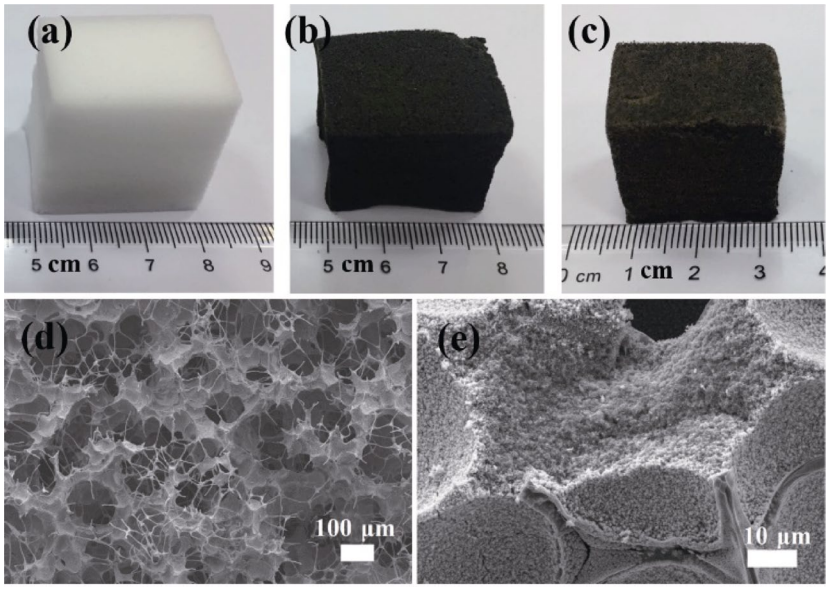

Fig. 6 (a) Photograph of one typical melamine foam. Photographs of the dried hybrid foams infiltrated with sols of (b) high viscosity and (c) low viscosity. (d) and (e) SEM images of the 1500 ℃-pyrolyzed foams impregnated with sols of viscosity 4.3 cP, 1500 ℃ in vacuum for 1 h [49]. Reproduced with permission from Ref. [49], © Springer Science+Business Media, LLC, part of Springer Nature 2018.

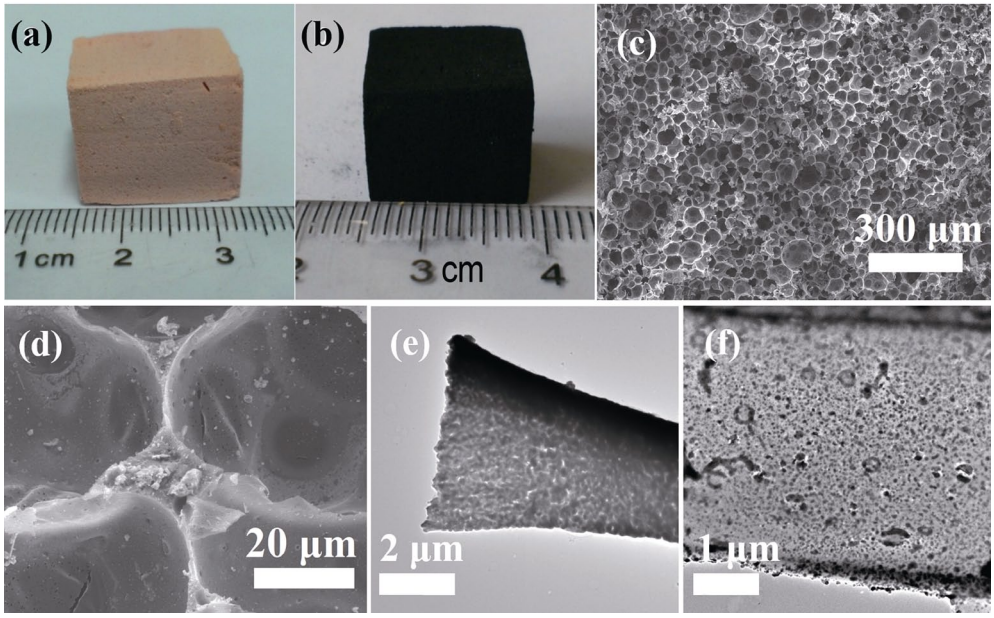

Fig. 7 (a) Photograph of the foamed green body and (b) ZrC/C foam obtained from pyrolysis at 1600 ℃ for 1 h. SEM images of ZrC/C foam after pyrolysis at 1600 ℃ with (c) low and (d) high magnification. TEM images of (e) the strut and (f) cell wall of ZrC/C foam after pyrolysis at 1600 ℃ [23]. Reproduced with permission from Ref. [23], © Elsevier Ltd. 2014.

83%–90%, respectively. The as-prepared ZrC foam showed spherical closed cell structures with average cell sizes about 40 μm, as shown in Figs. 7(c) and 7(d). The foamability of the mixtures originated from phenolic resin and it decreased as the zirconia sol content increased. It is difficult to precisely control carbon residue in the phenolic resin foaming derived porous ZrC/C. In the cell walls, ZrC particles were embedded in the continuous carbon matrix, as shown in Figs. 7(e) and 7(f). Carbon residue might hinder the ZrC grain growth at high temperatures, which might be one of the reasons why these ZrC/C foams displayed excellent thermal stability up to 2400 ℃.

Li *et al.* [25] developed a method to prepare stoichiometric ZrC foams by direct foaming of zirconia sols. Sucrose was used as carbon source and was dissolved into zirconia sol to get a viscous sol. The stabilization of the wet foam was based on the gelation of the zirconia sol under thermal aging. The microstructure of the ZrC foams can be tailored by controlling the foaming parameters, such as the viscosities of the sols, the concentration of the blowing and curing agents, which influenced the growth and stabilization of the bubbles in wet foam, as illustrated in Fig. 8. Pore sizes within the range of 40 to 500 μm have been achieved using this zirconia sol foaming method. The densities of the stoichiometric ZrC foams were in the range of 0.12–0.53 g/cm^3.

2. 4 Solvent evaporation methods

As described above, the sols are transformed into particulate gels that are established by van der Waals forces [46]. There are continuous liquid phase and solid phase in the wet gels. The solvent space between the solid network represents the potential pore space after drying [29,45]. In solvent evaporation methods, by forming a strengthened organic/inorganic interpenetrating network, the solvent is evaporated while the solid networks are preserved with limited shrinkage. By carbothermal conversion of interpenetrating metal oxide/resorcinol–formaldehyde (RF) nanoparticle networks, Leventis *et al*. [57] prepared monolithic HfC aerogels with diameter of 0.85 cm. The polymerization of RF sols and gelation of hydrated $HfCl_4$ with the help of epichlorohydrin occur in the same time scale, which leads to the formation of interpenetrating HfO_x/RF nanoparticle networks. By critical fluid (SCF) CO_2 drying of the wet gels followed with pyrolysis at 1400 ℃, HfC aerogels with porosity of 95% and average pore diameter of 22.9 nm are obtained. HfC xerogels with porosity of 44% and pore diameter of 3.1 nm are prepared by ambient pressure drying the wet gels. The morphologies of the HfC aerogels and xerogels are shown in Fig. 9.

To avoid cracking of the FA/zirconium oxychloride (ZOC)/TEOS hybrid gels during drying, Li *et al.* [21]

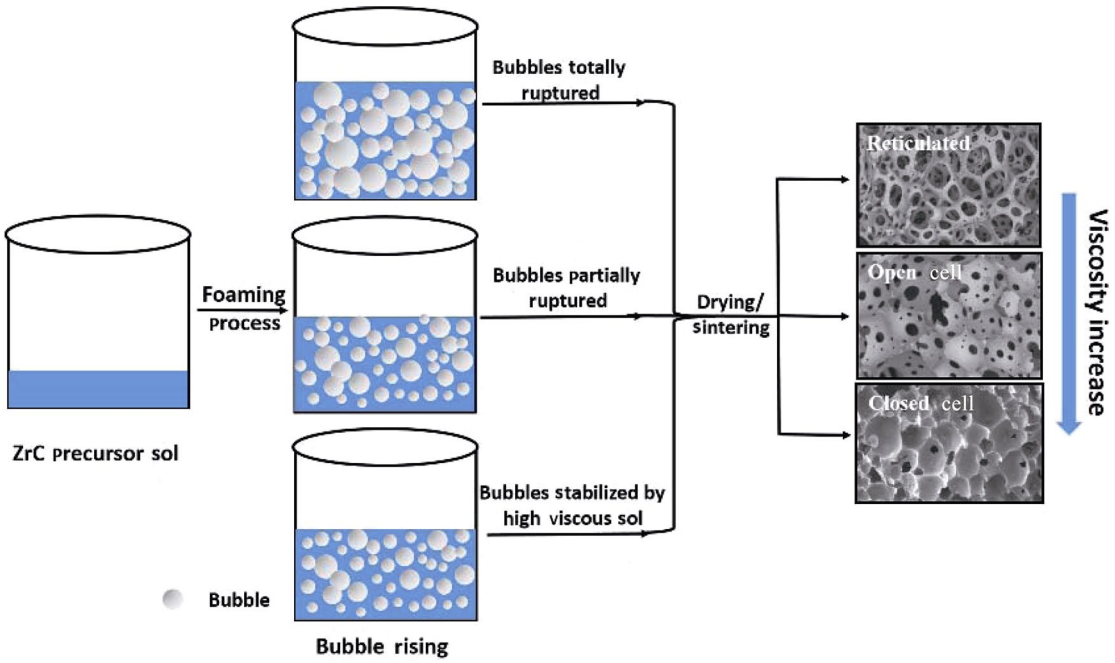

Fig. 8 Schematic illustration of the bubble growth and stabilization and the final microstructure of stoichiometric ZrC foams [25]. Reproduced with permission from Ref. [25], © Springer Science+Business Media New York 2015.

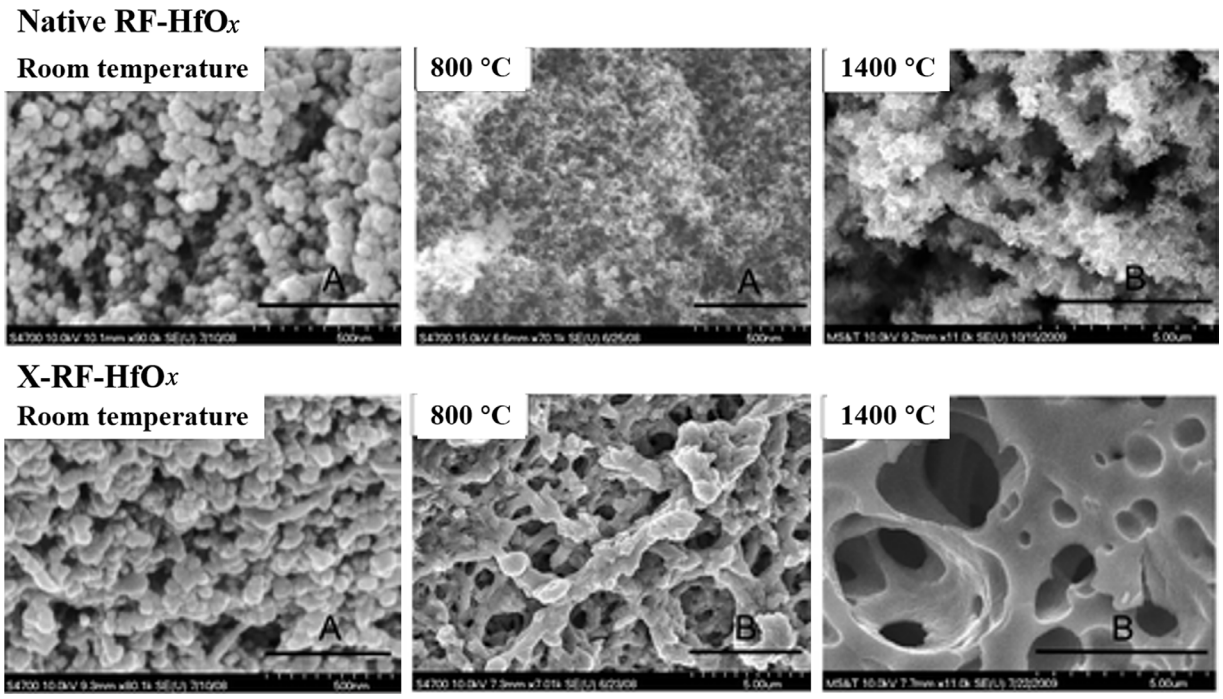

Fig. 9 Structural evolution by SEM upon pyrolysis (Ar, 3 h) of a representative RF-HfO_x system convertible to HfC. Scale bars: A, 500 nm; B, 5 μm [26]. Reproduced with permission from Ref. [26], © Elsevier Ltd and Techna Group S.r.l. 2016.

used polyethylene glycol (PEG) as phase separation inducing agent to prepare porous ZrC/SiC ceramics. PEG may strengthen the gel networks possibly by hydrogen bonding, and hence makes the porous networks robust enough to withstand the capillary forces during ambient pressure drying, as schematically illustrated in Fig. 10(a). Upon pyrolysis of the monolithic hybrid gels at temperatures above 1300 ℃, porous ZrC/SiC ceramics with porosities around 70% could be obtained. Simply by adjusting the PEG concentration in the starting

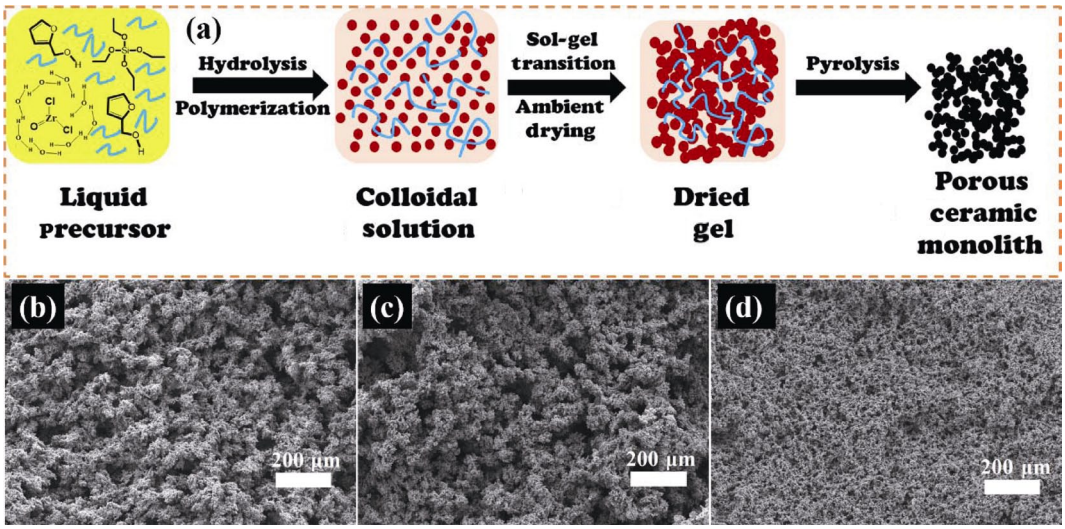

Fig. 10 (a) Schematic illustration for the preparation of porous ZrC/SiC ceramics with PEG as additive. SEM images of the porous ZrC/SiC ceramics with (b) low, (c) medium, and (d) high PEG concentration in the starting sol composition [21]. Reproduced with permission from Ref. [21], © Elsevier Ltd and Techna Group S.r.l. 2016.

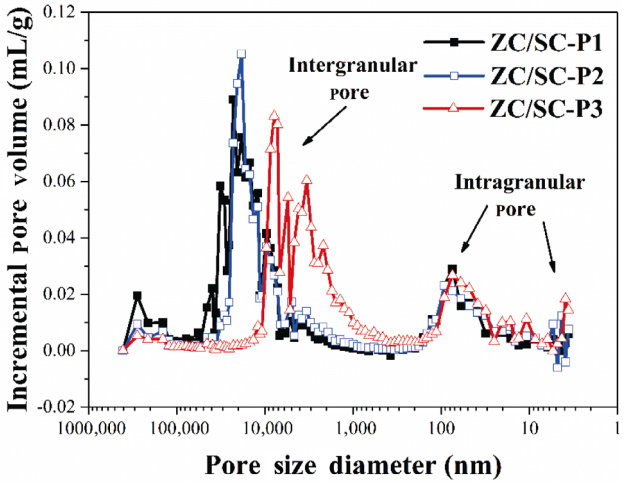

Fig. 11 Pore size distribution of the porous ZrC/SiC ceramics via solvent evaporation methods [21]. Reproduced with permission from Ref. [21], © Elsevier Ltd and Techna Group S.r.l. 2016.

composition, the morphology, pore sizes and their distribution, and mechanical properties of the porous ZrC/SiC can be tailored, as shown in Figs. 10(b), 10(c), and 11. The as-prepared porous ZrC/SiC ceramics are typical particulate gel structures and composed of spherical particles. These porous ZrC/SiC ceramics possess multimodal pore size distribution, distribution peaks in micron-sized range associated with voids between large clusters, and distribution peaks in nano-sized range associated with the pores within the spherical particles, as depicted in Fig. 11.

In the case of synthesizing transition metal boride-based porous ceramics, Li *et al.* [22] used FA, zirconium *n*-butoxide (ZTB), and boric acid as carbon, zirconium, and boron sources, respectively. By combining acid-catalyzed polymerization of FA and gelation of inorganic components, porous hybrid monoliths can be obtained by direct drying the wet gels under ambient pressure. Figures 12(a) and 12(b) demonstrate that these hybrid monoliths possess quite uniform porous morphology and have monomodal pore size distribution in the range from 0.3 to 3 μm. The hybrid monoliths composed of interconnected colloidal particles, whose sizes decrease with the increase of FA/Zr molar ratio. The porous structures composed of particle chains and narrow pore size distribution are well retained after ceramization at temperatures up to 1300–1600 ℃, as shown in Figs. 12(c)–12(f). In the case of FA/Zr equal to 3, the particle chains become fibrillar and the ceramic product shows typical reticulated porous structures (Fig. 12(e)). The ZrB_2-based porous ceramics via solvent evaporation method can reach porosity of 70%–85% and possess a monomodal pore size distribution between 1 and 10 μm.

3 Properties of the sol–gel derived porous UHTCs

Porous UHTCs are expected as promising candidate materials for the thermal protection systems of reusable launch and hypersonic vehicle [16,24]. These porous UHTCs must be lightweight and high temperature

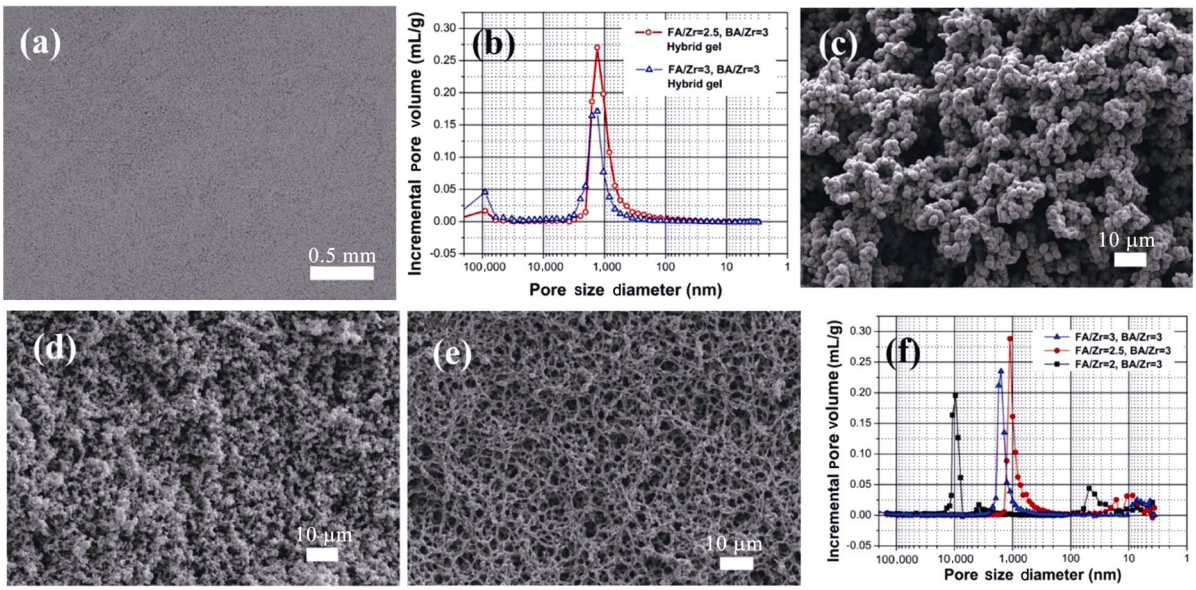

Fig. 12 (a) SEM image and (b) pore size distribution of the hybrid gels. SEM images and pore size distribution of the ZrB_2-based porous ceramics with various FA/Zr molar ratios: (c) FA/Zr = 2, (d) FA/Zr = 2.5, and (e) FA/Zr = 3 [22]. Reproduced with permission from Ref. [22], © Elsevier Ltd. 2017.

resistant, have a suitable mechanical integrity, low thermal conductivity, and be able to accommodate a complex geometry during the integration. Generally, the properties of the solid of which the cellular ceramic is made, the topology and shape of the cells, and the relative density of the cellular ceramic are three dominate factors that influence cellular properties [15]. However, in terms of sol–gel derived porous UHTCs, the papers are very limited, and few preliminary studies on compressive strength, high temperature resistance, and thermal conductivity have been carried out. The amount of the tested specimens is too small, and it is difficult to give out an overall view of the properties of the sol–gel derived porous UHTCs. We describe some case studies below for the properties of these materials.

3. 1 Compressive strength

Similar to many other porous oxide ceramics, the highly porous ZrC foams with spherical cell structures demonstrate huge strain before crushing, as depicted in Fig. 13(a) [23,25,37]. The stress–strain curve shows a linear elastic region followed by a plateau region, and ended with a densification region at large strain. Upon compression, the ZrC foam undergoes a progressive collapse of the cells and gives rise to the stress–strain plateau. Beyond the plateau, densification takes place and the stress rises sharply.

The stress–strain curves of the porous ZrB_2-based ceramics with interstitial voids between skeletal particles display a brittle fracture behavior, indicating

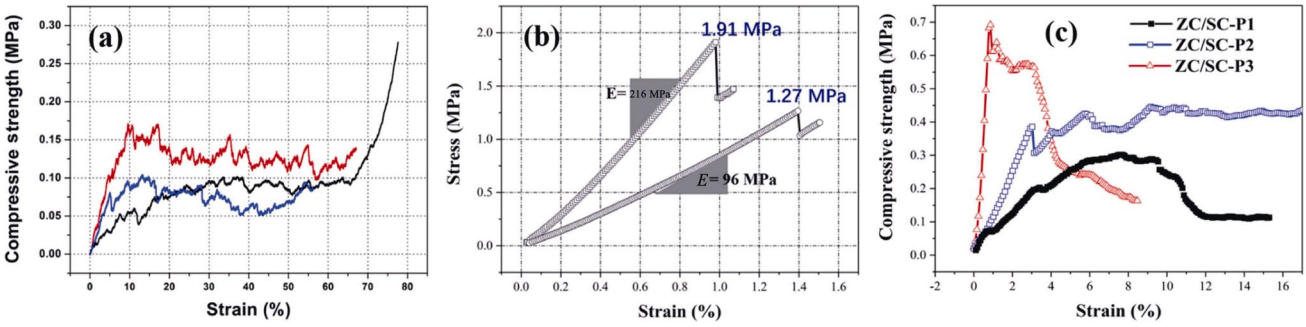

Fig. 13 Compressive stress–strain curves of the sol–gel derived porous UHTCs. (a) ZrC foams prepared by foaming method [37]. Reproduced with permission from Ref. [37], © IntechOpen 2019. (b) Porous ZrB_2/ZrC/SiC ceramics prepared by solvent evaporation method [22]. Reproduced with permission from Ref. [22], © Elsevier Ltd. 2017. (c) Porous ZrC/SiC ceramics prepared by solvent evaporation method [21]. Reproduced with permission from Ref. [21], © Elsevier Ltd and Techna Group S.r.l. 2016.

an elastic behavior up to a sudden rupture upon compression, as shown in Fig. 13(b) [22]. These rigid particle chains cannot withstand compressive loading through deformation, and hence display brittle fracture behavior upon external loading.

The compressive behavior of the sol–gel derived porous UHTCs demonstrates strong dependence on their microstructures (particle connectivity) [21]. Figure 13(c) shows the compressive stress–strain curves of the porous ZrC/SiC via solvent evaporation method. The porous ZrC/SiC ceramics composed of larger clusters of spherical particles which are less tightly connected have elastic and plateau region in their stress–strain curves. While those porous ZrC/SiC ceramics composed of tightly bounded particles demonstrate brittle fracture behavior. These results confirm that the topology of the porous UHTCs are important factors and can be used to tailor their mechanical properties.

3. 2 High-temperature stability

The difference in potential application temperature is one of the important features that distinguishes UHTCs from conventional ceramics. Porous UHTCs are expected to be used as thermal insulators at extreme high temperatures above 2000 ℃. The high temperature stability is one of the key properties to evaluate the overall performance of the porous UHTCs. Li *et al.* [22,23] studied the high-temperature macroscopic dimensional and microstructure stability of the ZrC/C foam and ZrB_2-based porous ceramics by thermal aging these ceramics at temperatures from 2000 to 2400 ℃ in inert atmosphere. These sol–gel derived porous UHTCs are sintering resistant and possess excellent high-temperature stability. After aged at 2000–2400 ℃, no obvious geometric changes or structural damages are detected. The microstructures of the ZrB_2-based porous ceramics are very stable and no coarse-grained morphology is observed after thermal aging at 2000 ℃ for 1 h, as shown in Fig. 14. Carbon residue, which may hinder grain growth at high-temperature aging, might be one of the key factors that give rise to high-temperature stability of these porous UHTCs.

3. 3 Thermal conductivity

Few papers reported the thermal properties of the sol–gel derived porous UHTCs. Li *et al.* [23] measured the thermal conductivity of the closed cell ZrC/C foam with porosity of 85% and the average pore size of 40 μm, as depicted in Fig. 15. Its thermal conductivity at 50 ℃ is 0.96 W/(m·K) and increases rapidly in the temperature from 50 to 200 ℃, and then reaches a plateau at 300 ℃ with thermal conductivity of 1.36 W/(m·K). A combined thermal conductivity of around 5 W/(m·K) is generally recommended for aerospace applications [16,63]. This closed cell ZrC/C foam is promising candidate material for aerospace with excellent high-temperature resistance.

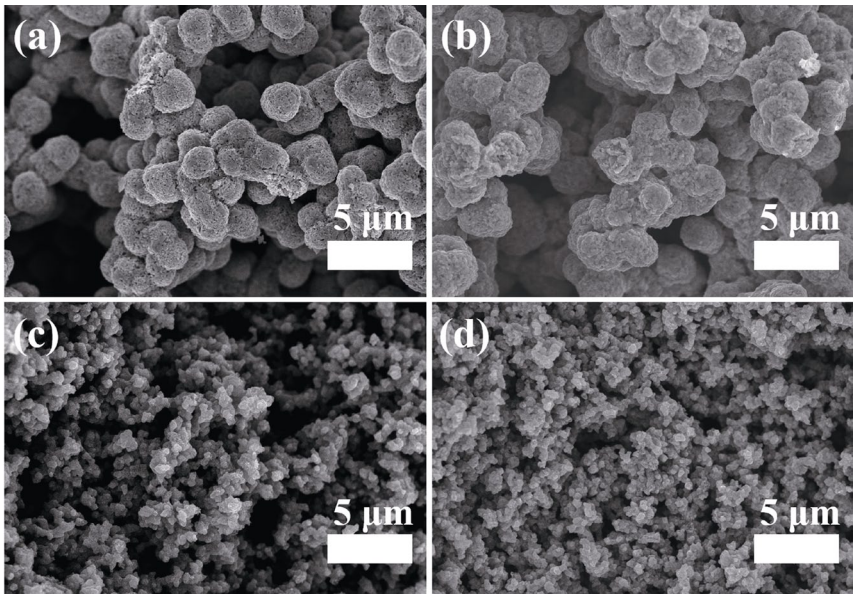

Fig. 14 SEM images of the porous ZrB_2/ZrC/SiC ceramics via solvent evaporation method before and after thermal aging at 2000 ℃ for 1 h [22]. Reproduced with permission from Ref. [22], © Elsevier Ltd. 2017.

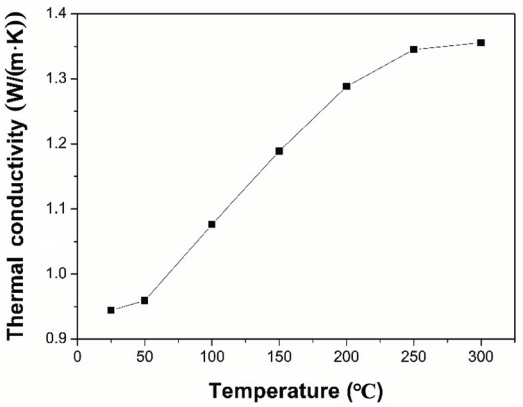

Fig. 15 Temperature dependence of thermal conductivity of the closed cell ZrC/C foams prepared by foaming methods [23]. Reproduced with permission from Ref. [23], © Elsevier Ltd. 2014.

4 Summary and outlook

Several sol–gel based processing routes using templating, foaming, and solvent evaporation are nowadays available for the production of porous UHTCs. The sol–gel methods for porous UHTCs involve the synthesis of liquid precursors, shaping the precursors to get green body, and heating at high temperatures to complete the ceramization. The key for all of these synthetic methods is pore designing.

In templating methods, the porous structure originates from the porous template. It is possible to produce a wide variety of porous UHTCs by this templating method. By impregnating/infiltrating the liquid precursors, followed by drying, and pyrolysis at 1300–1600 ℃, the porous UHTCs with pore sizes ranging from 10 to 200 μm at porosity levels of 80% can be produced. The rheology of the impregnating sol and its adhesion on the template are key issues in templating methods. It is important to keep in mind that high residue carbon content can be introduced into the final porous UHTCs if wood-derived carbon is chosen as the template.

In foaming methods, the porous structure originates from the generation and stabilization of the gas bubbles. By introducing the gas bubbles or volatile chemicals to the sol, followed by thermal setting or gelation of the sol, and heating at 1500–1600 ℃, the porous UHTCs with typical spherical cell structures of porosity ranging from 60% to 95% and cell sizes varying from 40 to 500 μm can be obtained. The open cell and closed cell structures of the porous UHTCs can be tailored by balancing the bubble growth and stabilization.

In solvent evaporation methods, the pores are generated by evaporating the solvent between the solid network. The key issue in these methods is how to avoid cracking and large volume shrinkage during drying. Supercritical fluid drying, surface modification, and the formation of interpenetrated particle networks have been used to weaken the capillary forces during drying process to obtain monolithic samples. By supercritical fluid drying the wet gel followed with high-temperature pyrolysis, HfC aerogels with average pore sizes of 22.9 nm and porosities over 95% can be obtained. Porous UHTCs with pore sizes ranging from 1 to 20 μm and porosities ranging from 65% to 85% can be produced by carbothermal conversion of the ambient pressure dried interpenetrated particles networks.

Application oriented studies of the sol–gel derived porous UHTCs are very limited. Porous UHTCs may be considered as good candidates for thermal protection systems used in extreme high temperatures. Sol–gel derived porous UHTCs demonstrate excellent high temperature stability and are sintering resistant at temperatures up to 2000–2400 ℃. The compressive strength of the porous UHTCs can reach up to 1.9 MPa with porosities over 80%. Thermal conductivity of the ZrC/C foam is about 1 W/(m·K) at 25 ℃ and increases with the increasing temperature. The preliminary studies of the properties of these sol–gel derived porous UHTCs show that they are promising materials for extreme high temperature applications, such as thermal protection systems of reusable launch and hypersonic vehicles. However, systematical studies to characterize the mechanical, thermal conductivity, thermal shock resistance, and thermal expansion properties of these porous UHTCs are needed.

Due to limited researches in sol–gel derived porous UHTCs, a detailed study to reveal the processing–structure–property relations for each of the main processing routes is still required. We hope that more progress will be made in the future by excellent research contributions. The systematical study would lead to significant advance not only in the precursor synthesis area, but also on the preparation of ultra-high temperature ceramic matrix composites for extreme applications.

Acknowledgements

Financial support from the National Natural Science

Foundation of China (Nos. 51602324 and 51532009) and the Fundamental Research Funds for the Central Universities (No. 2232018D3-32) are gratefully acknowledged.

References

[1] Zhang GJ, Ni DW, Zou J, *et al*. Inherent anisotropy in transition metal diborides and microstructure/property tailoring in ultra-high temperature ceramics—A review. *J Eur Ceram Soc* 2018, **38**: 371–389.

[2] Bao WC, Robertson S, Liu JX, *et al*. Structural integrity and characteristics at lattice and nanometre levels of ZrN polycrystalline irradiated by 4 MeV Au ions. *J Eur Ceram Soc* 2018, **38**: 4373–4383.

[3] Lu Y, Zou J, Xu FF, *et al*. Volatility diagram of ZrB_2-SiC-ZrC system and experimental validation. *J Am Ceram Soc* 2018, **101**: 3627–3635.

[4] Ji Z, Rubio V, Binner J. Thermoablative resistance of ZrB_2-SiC-WC ceramics at 2400 ℃. *Acta Mater* 2017, **133**: 293–302.

[5] Zhang GJ, Deng ZY, Kondo N, *et al*. Reactive hot pressing of ZrB_2-SiC composites. *J Am Ceram Soc* 2004, **83**: 2330–2332.

[6] Fahrenholtz WG, Hilmas GE. Ultra-high temperature ceramics: Materials for extreme environments. *Scr Mater* 2017, **129**: 94–99.

[7] Wuchina E, Opeka M, Causey S, *et al*. Designing for ultrahigh-temperature applications: The mechanical and thermal properties of HfB_2, HfC_x, HfN_x and αHf(N). *J Mater Sci* 2004, **39**: 5939–5949.

[8] Opeka MM, Talmy IG, Wuchina EJ, *et al*. Mechanical, thermal, and oxidation properties of refractory hafnium and zirconium compounds. *J Eur Ceram Soc* 1999, **19**: 2405–2414.

[9] Paul A, Jayaseelan DD, Venugopal S, *et al*. UHTC composites for hypersonic applications. *American Ceramic Society Bulletin* 2012, **91**: 22–29.

[10] Justin JF, Jankowiak A. Ultra high temperature ceramics: densification, properties and thermal stability. *Aerosp J* 2011: 1–11.

[11] Krishnarao RV, Bhanuprasad VV, Madhusudhan Reddy G. ZrB_2–SiC based composites for thermal protection by reaction sintering of ZrO_2+B_4C+Si. *J Adv Ceram* 2017, **6**: 320–329.

[12] Gui KX, Liu FY, Wang G, *et al*. Microstructural evolution and performance of carbon fiber-toughened ZrB_2 ceramics with SiC or $ZrSi_2$ additive. *J Adv Ceram* 2018, **7**: 343–351.

[13] He RJ, Qu ZL, Liang D. Rapid heating thermal shock study of ultra high temperature ceramics using an *in situ* testing method. *J Adv Ceram* 2017, **6**: 279–287.

[14] Fahrenholtz WG, Wuchina EJ, Lee WE, *et al*. *Ultra-high Temperature Ceramics: Materials for Extreme Environment Applications*. Hoboken (USA): John Wiley & Sons, Inc., 2014.

[15] Scheffler M, Colombo P. *Cellular Ceramics: Structure, Manufacturing, Properties and Applications*. New York: Wiley-VCH Verlag GmbH & Co. KGaA, 2005.

[16] Tallon C, Franks GV. Multi-scale porous ultra-high temperature ceramics. Final project report. Sponsored by Asian Office of Aerospace Research and Development. Grant Number: AOARD-134068. 2015: 43.

[17] Du JC, Zhang XH, Hong CQ, *et al*. Microstructure and mechanical properties of ZrB_2–SiC porous ceramic by camphene-based freeze casting. *Ceram Int* 2013, **39**: 953–957.

[18] Landi E, Sciti D, Melandri C, *et al*. Ice templating of ZrB_2 porous architectures. *J Eur Ceram Soc* 2013, **33**: 1599–1607.

[19] Sani E, Mercatelli L, Sans JL, *et al*. Porous and dense hafnium and zirconium ultra-high temperature ceramics for solar receivers. *Opt Mater* 2013, **36**: 163–168.

[20] Jin XX, Dong LM, Li Q, *et al*. Thermal shock cracking of porous ZrB_2-SiC ceramics. *Ceram Int* 2016, **42**: 13309–13313.

[21] Li F, Wang XG, Huang X, *et al*. Preparation of ZrC/SiC porous self-supporting monoliths via sol–gel process using polyethylene glycol as phase separation inducer. *J Eur Ceram Soc* 2018, **38**: 4806–4813.

[22] Li F, Huang X. Preparation of highly porous ZrB_2/ZrC/SiC composite monoliths using liquid precursors via direct drying process. *J Eur Ceram Soc* 2018, **38**: 1103–1111.

[23] Li F, Kang Z, Huang X, *et al*. Preparation of zirconium carbide foam by direct foaming method. *J Eur Ceram Soc* 2014, **34**: 3513–3520.

[24] Fahrenholtz WG, Hilmas GE. Ultra-high temperature ceramics: Materials for extreme environments. *Scr Mater* 2017, **129**: 94–99.

[25] Li F, Liang MS, Ma XF, *et al*. Preparation and characterization of stoichiometric zirconium carbide foams by direct foaming of zirconia sols. *J Porous Mater* 2015, **22**: 493–500.

[26] Jin XX, Dong LM, Xu HY, *et al*. Effects of porosity and pore size on mechanical and thermal properties as well as thermal shock fracture resistance of porous ZrB_2-SiC ceramics. *Ceram Int* 2016, **42**: 9051–9057.

[27] Medri V, Mazzocchi M, Bellosi A. ZrB_2-based sponges and lightweight devices. *Int J Appl Ceram Technol* 2011, **8**: 815–823.

[28] Franks GV, Tallon C, Studart AR, *et al*. Colloidal processing: Enabling complex shaped ceramics with unique multiscale structures. *J Am Ceram Soc* 2017, **100**: 458–490.

[29] Feinle A, Elsaesser MS, Hüsing N. Sol–gel synthesis of monolithic materials with hierarchical porosity. *Chem Soc Rev* 2016, **45**: 3377–3399.

[30] Okada K, Isobe T, Katsumata KI, *et al*. Porous ceramics mimicking nature—Preparation and properties of microstructures with unidirectionally oriented pores. *Sci Technol Adv Mater* 2011, **12**: 064701.

[31] Studart AR, Gonzenbach UT, Tervoort E, *et al*. Processing routes to macroporous ceramics: A review. *J Am Ceram Soc* 2006, **89**: 1771–1789.
[32] Colombo P. In praise of pores. *Science* 2008, **322**: 381–383.
[33] Qian YB, Zhang WG, Ge M, *et al*. Frictional response of a novel C/C-ZrB_2-ZrC-SiC composite under simulated braking. *J Adv Ceram* 2013, **2**: 157–161.
[34] Guo XZ, Cai XB, Zhu L, *et al*. Preparation and properties of SiC honeycomb ceramics by pressureless sintering technology. *J Adv Ceram* 2014, **3**: 83–88.
[35] Wu JM, Zhang XY, Xu J, *et al*. Preparation of porous Si_3N_4 ceramics via tailoring solid loading of Si_3N_4 slurry and Si_3N_4 poly-hollow microsphere content. *J Adv Ceram* 2015, **4**: 260–266.
[36] Wu HB, Yin J, Liu XJ, *et al*. Aqueous gelcasting and pressureless sintering of zirconium diboride foams. *Ceram Int* 2014, **40**: 6325–6330.
[37] Li F, Huang X, Zhang GJ. Preparation of ultra-high temperature ceramics-based materials by sol–gel routes. In *Recent Applications in Sol-gel Synthesis*. Usha C, Ed. InTech, 2017.
[38] Danks AE, Hall SR, Schnepp Z. The evolution of 'sol–gel' chemistry as a technique for materials synthesis. *Mater Horiz* 2016, **3**: 91–112.
[39] Nakanishi K, Kanamori K, Tokudome Y, *et al.* Sol–gel processing of porous materials. In *Handbook of Solid State Chemistry*. Dronskowshi R, Kikkawa S, Stein A, Eds. New York: Wiley-VCH Verlag GmbH & Co. KGaA, 2017.
[40] Sacks MD, Wang CA, Yang ZH, *et al*. Carbothermal reduction synthesis of nanocrystalline zirconium carbide and hafnium carbide powders using solution-derived precursors. *J Mater Sci* 2004, **39**: 6057–6066.
[41] Dollé M, Gosset D, Bogicevic C, *et al*. Synthesis of nanosized zirconium carbide by a sol–gel route. *J Eur Ceram Soc* 2007, **27**: 2061–2067.
[42] Yan CL, Liu RJ, Cao YB, *et al*. Carbothermal synthesis of submicrometer zirconium carbide from polyzirconoxane and phenolic resin by the facile one-pot reaction. *J Am Ceram Soc* 2012, **95**: 3366–3369.
[43] Ang CE, Williams T, Seeber A, *et al*. Synthesis and evolution of zirconium carbide via sol–gel route: Features of nanoparticle oxide-carbon reactions. *J Am Ceram Soc* 2013, **96**: 1099–1106.
[44] Cai T, Qiu WF, Liu D, *et al.* Synthesis of ZrC–SiC powders by a preceramic solution route. *J Am Ceram Soc* 2013, **96**: 3023–3026.
[45] Ziegler C, Wolf A, Liu W, *et al.* Modern inorganic aerogels. *Angew Chem Int Ed* 2017, **56**: 13200–13221.
[46] Brinker CJ, Scherer GW. *Sol-Gel Science: The Physics and Chemistry of Sol-Gel Processing*. San Diego (USA): Academic Press Inc., 1990.
[47] Ji ZH, Ye L, Tao XY, *et al.* Synthesis of ordered mesoporous ZrC/C nanocomposite via magnesiothermic reduction at low temperature. *Mater Lett* 2012, **71**: 88–90.
[48] Brinker CJ, Scherer GW. Drying. In *Sol-Gel Science*. Brinker CJ, Scherer GW, Eds. San Diego (USA): Academic Press, 1990: 452–513.
[49] Li F, Bao WC, Ni DW, *et al*. A thermoset hybrid sol for the syntheses of zirconium carbide–silicon carbide foam via replica method. *J Porous Mater* 2019, **26**: 409–417.
[50] Nakanishi K, Tanaka N. Sol–gel with phase separation. Hierarchically porous materials optimized for high-performance liquid chromatography separations. *Acc Chem Res* 2007, **40**: 863–873.
[51] Basnet B, Sarkar N, Park JG, *et al*. Al_2O_3–TiO_2/ZrO_2–SiO_2 based porous ceramics from particle-stabilized wet foam. *J Adv Ceram* 2017, **6**: 129–138.
[52] Krivoshapkina EF, Krivoshapkin PV, Vedyagin AA. Synthesis of Al_2O_3–SiO_2–MgO ceramics with hierarchical porous structure. *J Adv Ceram* 2017, **6**: 11–19.
[53] Rambo CR, Cao J, Rusina O, *et al*. Manufacturing of biomorphic (Si, Ti, Zr)-carbide ceramics by sol–gel processing. *Carbon* 2005, **43**: 1174–1183.
[54] Venugopal S, Boakye EE, Paul A, *et al*. Sol-gel synthesis and formation mechanism of ultrahigh temperature ceramic: HfB_2. *J Am Ceram Soc* 2014, **97**: 92–99.
[55] Tao XY, Qiu WF, Li H, *et al*. Synthesis of nanosized zirconium carbide from preceramic polymers by the facile one-pot reaction. *Polym Adv Technol* 2010, **21**: 300–304.
[56] Li F, Huang X, Zhang GJ. Scalable foaming assisted synthesis of ZrC nanopowder by carbothermal reduction. *Ceram Int* 2015, **41**: 3335–3338.
[57] Leventis N, Chandrasekaran N, Sadekar AG, *et al*. The effect of compactness on the carbothermal conversion of interpenetrating metal oxide/resorcinol-formaldehyde nanoparticle networks to porous metals and carbides. *J Mater Chem* 2010, **20**: 7456–7471.
[58] Jin XX, Zhang XH, Han JC, *et al*. Thermal shock behavior of porous ZrB_2–SiC ceramics. *Mater Sci Eng* 2013, **588**: 175–180.
[59] Schwartzwalder K, Somers H, Somers AV. Method of making porous ceramic articles. U.S. patent 3 090 094, May 1963.
[60] Gonzenbach UT, Studart AR, Tervoort E, *et al*. Ultrastable particle-stabilized foams. *Angew Chem Int Ed* 2006, **45**: 3526–3530.
[61] Gonzenbach UT, Studart AR, Tervoort E, *et al*. Tailoring the microstructure of particle-stabilized wet foams. *Langmuir* 2007, **23**: 1025–1032.
[62] Gonzenbach UT, Studart AR, Tervoort E, *et al*. Stabilization of foams with inorganic colloidal particles. *Langmuir* 2006, **22**: 10983–10988.
[63] Zhang S, Zhao DL. *Aerospace Materials Handbook*. Boca Raton (USA): CRC Press, 2012.